DOI: 10.1002/cbic.200700670

Theoretical and Experimental Evaluation of a CYP106A2 Low Homology Model and Production of Mutants with Changed Activity and Selectivity of Hydroxylation

Michael Lisurek,[a] Birgit Simgen,[a] Iris Antes,[b] and Rita Bernhardt*[a]

Steroids are important pharmaceutically active compounds. In contrast to the liver drug-metabolising cytochrome P450s, which metabolise a variety of substrates, steroid hydroxylases generally display a rather narrow substrate specificity. It is therefore a challenging goal to change their regio- and stereoselectivity. CYP106A2 is one of only a few bacterial steroid hydroxylases and hydroxylates 3-oxo-Δ^4-steroids mainly in 15β-position. In order to gain insights into the structure and function of this enzyme, whose crystal structure is unknown, a homology model has been created. The substrate progesterone was then docked into the active site to predict which residues might affect substrate binding. The model was substantiated by using a combination of theoretical and experimental investigations. First, numerous computational structure evaluation tools assessed the plausibility of its protein geometry and its quality. Second, the model explains many key properties of common cytochrome P450s. Third, two sets of mutants have been heterologously expressed, and the influence of the mutations on the catalytic activity towards deoxycorticosterone and progesterone has been studied experimentally: the first set comprises six mutations located in the structurally variable regions of this enzyme that are very difficult to predict by cytochrome P450 modelling (K27R, I86T, E90V, I71T, D185G and I215T). For these positions, no participation in the active-site formation was predicted, or could be experimentally demonstrated. The second set comprises five mutants in substrate recognition site 6 (S394I, A395L, T396R, G397P and Q398S). For these residues, participation in active-site formation and an influence on substrate binding was predicted by docking. These mutants are based on an alignment with human CYP11B1, and in fact most of these mutants altered the active-site structure and the hydroxylation activity of CYP106A2 dramatically.

Introduction

Cytochrome P450s comprise a superfamily of enzymes that are mainly responsible for the hydroxylation of a wide variety of hydrophobic compounds.[1] Besides this, they catalyse reactions such as N-oxidation, N-, O- and S-dealkylation, sulfoxidation, epoxidation, peroxidation, deamination, desulfuration, dehalogenation and N-oxide reduction.[2,3] Whereas eukaryotic P450s are usually integral membrane proteins, the bacterial CYP106A2 from *Bacillus megaterium* ATCC 13368 is one of only a few cloned soluble steroid-converting cytochrome P450s. It hydroxylates 3-oxo-Δ^4-steroids like deoxycorticosterone (DOC) and progesterone (P) mainly at the 15β-position.[4] In the case of P as a substrate, 6β-,[4,5] 9α- and 11α-hydroxylation were also reported.[6] Some of these monohydroxylated Ps, including their derivatives are known as pharmaceuticals or useful intermediates in the production of a number of pharmaceutically active compounds.[7–10] A long-sought practical goal in cytochrome P450 research is to capitalise on the exquisite specificity of these enzymes in regio- and stereoselective hydroxylation reactions for the production of chemicals that are difficult to prepare by using traditional organic synthesis methods, especially in the case of steroids. The prerequisite for rational engineering of enzymes is, however, the knowledge of their structure. Because numerous attempts to crystallise CYP106A2 have been unsuccessful so far,[11] a homology model has been created to gain deeper insights into the structure and function and—in a later step—for the rational design of mutants to influence the steroid hydroxylation directly as desired. In recent years, homology modelling has become a promising tool to study cytochrome P450 function. Whereas the number of modelled bacterial cytochrome P450 structures is rather low,[12–14] numerous mammalian cytochrome P450 homology models have been constructed, and the resulting structures were successfully evaluated in view of mutagenesis data (see, for example, refs. [15–18]).

Results and Discussion

Modelling and evaluation of CYP106A2

Modelling has been performed by using the SYBYL 6.7 subroutine COMPOSER.[19] The backbone coordinates for the core

[a] *M. Lisurek, B. Simgen, Prof. Dr. R. Bernhardt*
Universität des Saarlandes, FR 8.8 Biochemie
Gebäude 9, Im Stadtwald, 66041 Saarbrücken (Germany)
Fax: (+49) 681-302-4739
E-mail: ritabern@rz.uni-sb.de

[b] *Dr. I. Antes*
Max-Planck-Institut für Informatik
Computational Biology and Applied Algorithmics
Campus E14, 66123 Saarbrücken (Germany)

Supporting information for this article is available on the WWW under http://www.chembiochem.org or from the author.

structure of the model were built by using the set of 10 structurally conserved regions (SCRs) that were obtained by the structural alignment of CYP106A2 with five template cytochromes P450 (Figure 1). The scoring parameters of the pairwise sequence alignments are given in Table 1. A schematic

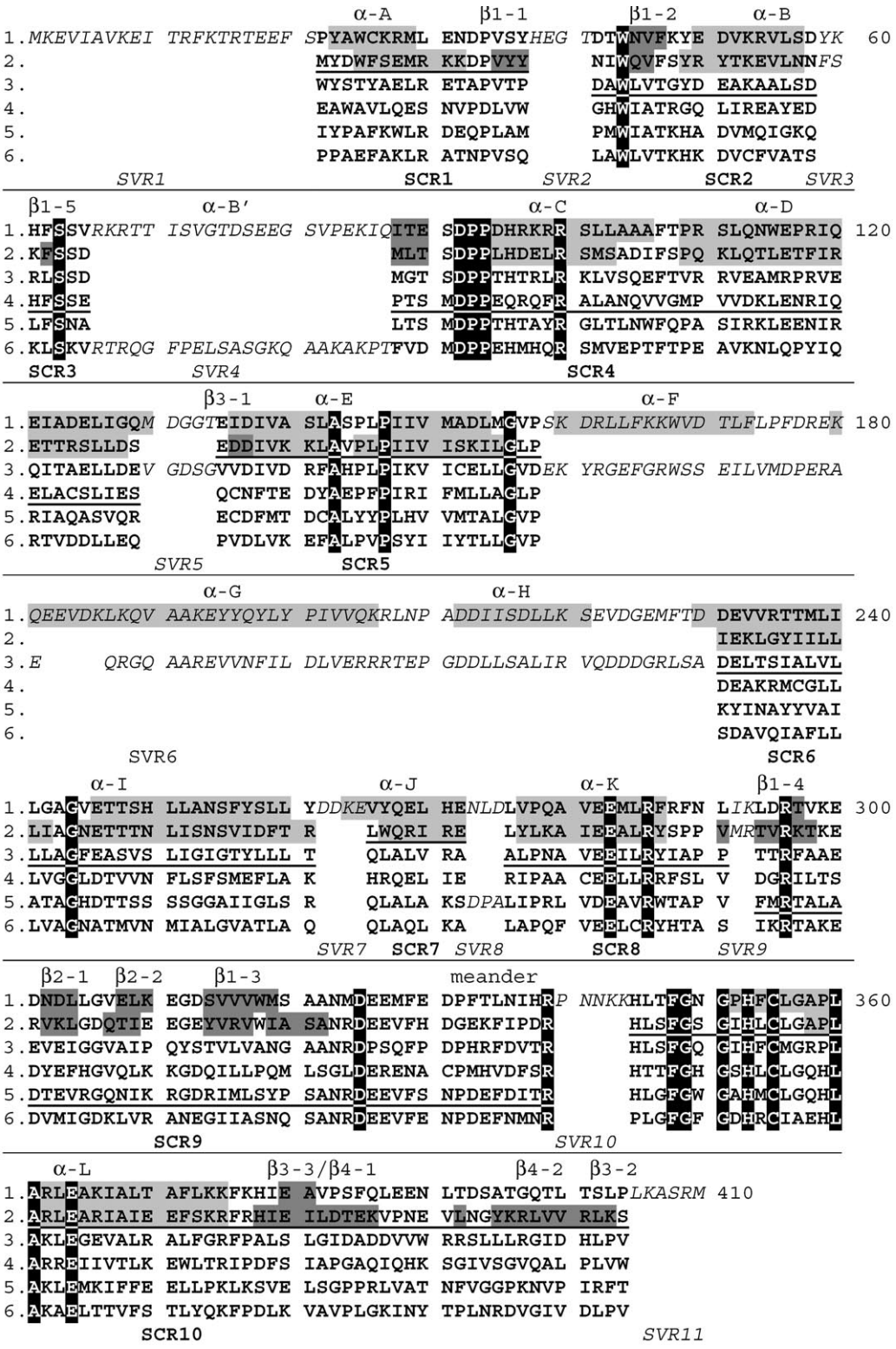

Figure 1. Composer alignment of CYP106A2 and the five template cytochrome P450s. 1, CYP106A2, 2, CYP119, 3, CYP107A1, 4, CYP101, 5, CYP108, 6, CYP55A1. The structurally conserved regions (SCRs) and the structurally variable regions (SVRs) of CYP106A2 are displayed in bold and in italic characters, respectively. The fragments used for building the SCRs are underlined. The absolutely conserved residues among the six proteins are labelled in black. The nomenclature of α helices (light grey) and β sheets (dark grey) shown above the sequences is according to Haseman et al.[22]

Table 1. Percentages of sequence identities and statistical significance scores. Percentages of sequence identities and statistical significance scores of CYP106A to the five template sequences of CYP119, CYP108, CYP107A1, CYP101 and CYP55A1 according to the PMUTATION.HOMO similarity matrix (see Experimental Section). The Protein Data Bank entry names are listed in brackets.

	Identity [%]	Significance score
CYP119 (1F4T)	32.2	20.3
CYP107A1 (1OXA)	28.5	19.0
CYP101 (1PHG)	27.1	15.5
CYP108 (1CPT)	26.8	18.8
CYP55A1 (1L6)	25.6	15.9

ribbon presentation of the modelled CYP106A2 structure is shown in Figure 2.

The good stereochemical quality of the model is shown in the Ramachandran plot (Figure 3A). The distribution of the

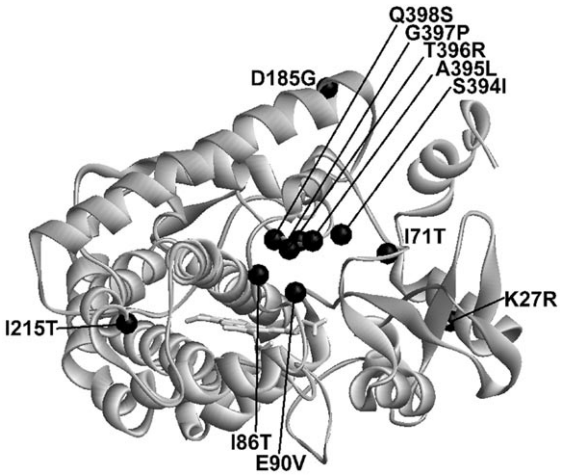

Figure 2. Ribbon representation of the tertiary structure of the CYP106A2 model. The incorporated haem is shown as light grey stick model. The Cα positions of the investigated mutations are shown as black balls and are labelled.

ϕ/ψ angles is well within the allowed regions. The majority (96%) of the residues are in the favoured regions of the plot; 78.8% of the residues are in the most favoured regions and 17.2% are in the additional allowed regions. The four residues in the disallowed region are found only in the loop regions near the surface of the model and are a result of the fusion of the SCRs to the structurally variable regions (SVRs). Therefore, the backbone conformation is of nearly as good reliability as those of the crystal structures. A validation check of the energetic properties was performed by using PROSA II.[20] The main criterion is that each residue interaction energy with the remainder of the protein should be negative. A comparison of the energy profiles of the modelled CYP106A2 and its most homologous template, CYP119 is shown in Figure 3B. According to this criterion, the reliability of the CYP106A2 model is similar to that of the solved crystal structures. Another criterion of this validation method is that the total energy of the protein

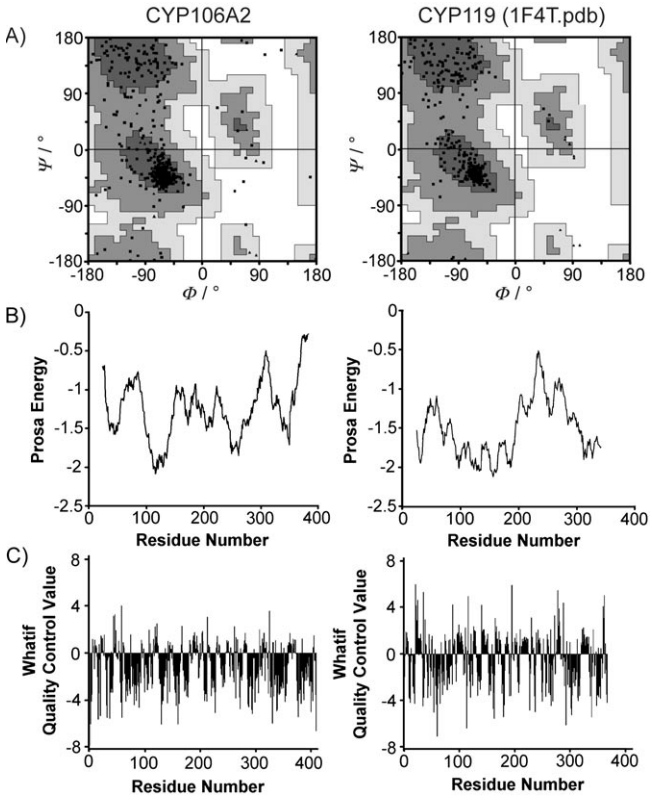

Figure 3. Comparison of the evaluation of the modelled CYP106A2 structure (left) and CYP119 (1F4T; right). A) Ramachandran plot of the Φ/Ψ distribution. The most favoured regions are represented in dark grey, additional allowed regions are grey, generously allowed regions are light grey and disallowed regions are white. Glycine residues are shown as triangles. B) PROSA II energy plot. The graphs are smoothed over a window size of 50 residues. The curves represent the residue interaction energies, negative values correspond to favourable interactions within the molecules. C) WHATIF quality control profile. The graphs represent the packing quality of each residue.

structure should be low, a property that is represented by the PROSA z-score.[20] The normalized *z*-score was calculated according to Chang and Loew.[13] PROSA *z*-scores and normalised z-scores are summarised in Table 2. The normalized z-score of 0.85 that was obtained for the model is almost comparable to the values obtained for the reference proteins; this clearly demonstrates that the model is of reliable quality. The next evaluation criterion was a comparison of the packing environment of the residues in the model with the average packing environment for the same residue types in crystal structures that are contained in the Protein Data Bank by using the WHATIF quality control method.[21] A residue in a structure with a score of -5.0σ or lower indicates poor packing, any involvement of this residue in active-site formation or contacts with a cofactor should be treated with scepticism. A comparison of the WHATIF quality control profile of the model and CYP119 is shown in Figure 3C. In CYP106A2, 16 residues are found that have a score $>$-5.0σ, compared to 8 in CYP119, 6 in CYP108, 8 in CYP101, 7 in CYP107A1 and 10 in CYP55A1. These results are comparable for the model and the crystal structures. To evaluate the overall quality of the model, the average quality control value was used. If the average quality control value is

Table 2. Evaluation of the CYP106A2 model in comparison to the five template structures. Results of PROSA II, PROCHECK and WHATIF quality control for the modelled CYP106A2 and the five template structures 1F4T, 1OXA, 1CPT, 1PHG and 1L6.

	Sequence Length[a]	PROCHECK overall score[b]	PROSA II *z*-score	PROSA II normalised *z*-score	WHATIF quality control value
CYP106A2	410	−0.50	−10.69	0.85	−1.36
1F4T	367	0.37	−12.17	1.01	−0.52
1OXA	403	0.36	−13.45	1.09	−0.55
1PHG	405	−0.32	−14.65	1.18	−0.49
1CPT	412	−0.18	−12.79	1.02	−0.78
1L6	399	0.38	−12.43	1.00	−0.55

below −3.0, the structure is unreliable. Values equal or above −1.5 indicate good structures. As presented in Table 2, the values for the template proteins are between −0.49 and −0.78. The average quality control value for CYP106A2 is −1.36, which indicates a good model. PROSA II energy profiles and WHATIF quality control profiles of other bacterial cytochrome P450s can be found elsewhere.[13]

The reliability of the model could also be shown by the finding that residues that are known to be invariant or highly conserved from investigations of solved structures are also conserved in CYP106A2.[22]

Haem binding

The haem-binding region is one of the most conserved regions among cytochrome P450 structures. According to the model, in CYP106A2 the A-ring propionic acid interacts in a bidentate fashion with R296 (R259 in CYP119), the D-ring propionic acid interacts with H96, H353 and R100 (H76, H315 and R80 are the corresponding residues in CYP119).

Catalysis

There is a strongly conserved acidic residue followed by a strongly conserved threonine in the middle of the I-helix in most cytochrome P450s (E246 and T247 in CYP106A2, E212 and T213 in CYP119). The corresponding threonine in CYP101 (T252) was shown to be involved in proton delivery to iron-bound molecular oxygen,[23] and in CYP119, T213 is followed by two additional threonines. In CYP106A2 T247 is also present in the active site adjacent to the haem and is followed by one additional threonine and a serine (T248 and S249). Both T213 and T214, have been mutated in CYP119, and the mutants exhibited dramatic changes in both spin state and catalysis.[24,25] It might well be speculated that in CYP106A2, as in CYP119, the H-bonding network that involves these threonine and serine residues in the I-helix is also involved in the proton shuttle that is important for proton delivery and molecular oxygen activation.

Redox–partner binding

Experimental evidence suggested that cytochrome P450s interact with their electron donor at the proximal site of the molecule. Negatively charged amino acids on the electron donor are critical for proper interactions,[26–30] whereas the cytochrome P450 provides the positively charged residues.[31,32] A common region of positive charges is centred over the cysteine-pocket of all bacterial type 1 cytochrome P450s that interact with ferredoxins. In order to identify the surface residues of CYP106A2 that are responsible for the redox–partner interaction, the model of CYP106A2 was compared with CYP101, because this cytochrome P450 has been studied most intensively. Three surface arginine residues on the proximal site of CYP101 were identified as necessary for successful electron transfer from putidaredoxin.[33] These residues are R72 in the B-helix, and R109 and R112 in the C-helix.[34–36] R112 has additionally been discussed to be involved in electron transfer.[37] There are corresponding positively charged residues in the CYP106A2 model, namely K53, R97 and R100. Additionally, R364 in the L-helix of CYP101 has been discussed to contribute to putidaredoxin binding.[38] The corresponding position in CYP106A2 is R362. Taken together, a patch of positively charged residues is located on the surface of CYP106A2 in homologous positions to those shown to be involved in redox partner binding in CYP101.

Stability

With 368 residues, CYP119 is considerably shorter than CYP106A2, which has 410 residues. A difference of 21 amino acids is located at the N terminus. CYP106A2 has an extra helix (A′) that does not exist in CYP119. The remainder of the differences in length occur primarily in the surface turns. The structure of the so-called meander is stabilized by the highly conserved ERR triad. This salt-bridge network is formed by a glutamate and an arginine in the K-helix and an arginine from the meander region. According to the model presented herein, the ERR triad of CYP106A2 is formed by E283, R286 and R339. Besides the residues mentioned above, when using the nomenclature of CYP101, also G60, G249, F350, G353, H355, C357, G359, A363 and L375 are considered to be highly conserved.[39] Because their existence has been shown to be important in maintaining protein function and stability in CYP101, they are also expected to be conserved in other cytochrome P450s. As can be seen in Figure 1, all these residues are also absolutely conserved in CYP106A2, except for G40 of CYP106A2, which is shifted by one residue with respect to G60 of CYP101. The *cis* prolyl–prolyl peptide that is seen in all five template structures is also present in the CYP106A2 model between P93 and P94.

Docking and alignment

In order to rationalize substrate binding, P was docked and energy minimized in the active site of the model. The five

favourable docking solutions with the lowest energy scores exhibited at least one hydrogen bond between the C3 keto group of P and the A395 to T396 loop (either to the backbone amides of A395 or T396 or the hydroxy group of T396; Figure 4). This result points directly to the importance of these residues and their environment for substrate binding. In addition, these residues lie within the putative substrate recognition site (SRS) 6[40] and were therefore chosen for the following mutagenesis studies to create mutants with altered hydroxylation activity. No specific interactions with other SRSs were observed. CYP11B1 was chosen as a second template because the two steroid hydroxylases, CYP106A2 and CYP11B1, both produce pharmaceutically interesting steroid hormones. The overall sequence identity between these only sparsely related enzymes is less than 20%. The alignment between CYP106A2 and human CYP11B1 in the putative SRS 6, including the preceding conserved L-helix and the succeeding C terminus is shown in Figure 5. Five mutants in SRS 6 (S394I, A395L, T396R, G397P and Q398S) have been produced in which the residues that are found in CYP106A2 have been changed to those that are found in CYP11B1. This way, a change in the activity and regiospecificity of hydroxylation from the 15 to the 11-position was expected to occur. In control experiments, residues of CYP106A2 that are located in the SVRs and on the surface of the protein have been replaced. According to the model, mutations I71T, I86T and E90V are situated in the B′-helix of CYP106A2 and its adjacent loops. D185G is in the loop between the F and the G-helix and could play a role in substrate access to the active site.[41] K27R is placed in the putative A-helix and I215T is located on the surface of the enzyme in the H-helix (Figure 2). These mutants were chosen because the B′-helix and its adjacent loops, besides the F/G-loop are some of the most variable regions in cytochrome P450 structures.[13,42,43] However, no participation in substrate binding is predicted for these residues according to the model.

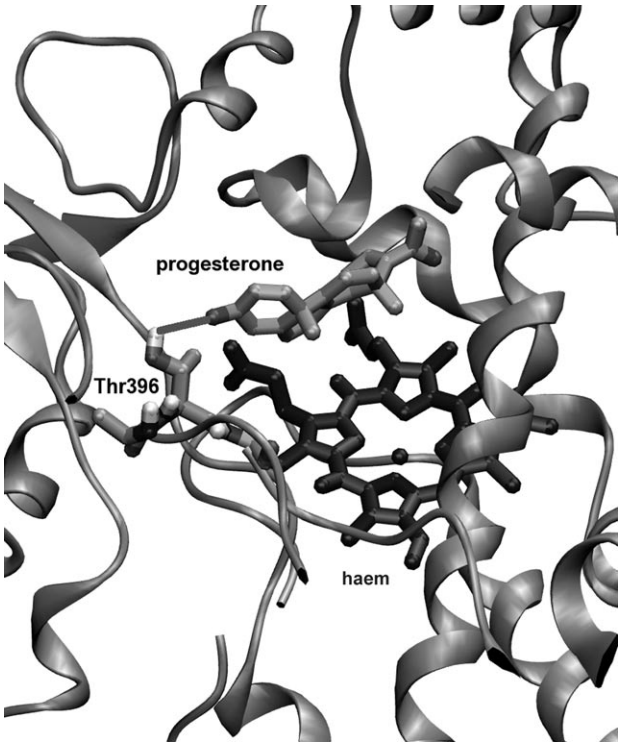

Figure 4. The binding pocket of CYP106A2 with the substrate progesterone. The substrate, the haem-cofactor and the loop A395–G397 are drawn in stick representation and the hydrogen bond between the substrate and T396 is shown.

Expression and purification of recombinant CYP106A2 and the mutants

By using our previously established purification procedure,[6] about 6900 nmol (~300 mg) holoenzyme WT-CYP106A2 could be purified per litre *Escherichia coli* culture. On the SDS-gel, WT-CYP106A2 appears as protein with an apparent mass of 47 kDa and the isoelectric point was determined to be 4.9 (data not shown). The mutants were constructed by site-directed mutagenesis, confirmed by nucleotide sequencing and expressed with the same system as WT-CYP106A2. All mutants could be purified to homogeneity as judged by SDS polyacrylamide gel electrophoresis (data not shown), by a purity index (A_{417}/A_{279}) of the proteins of about 1.7–1.9 and a cytochrome P450-to-protein ratio of approximately 21 nmol per mg protein.

Spectral characterisation of WT-CYP106A2 and the mutants

To determine the effect of the amino acid replacements in the putative SRS 6 in the variable regions on the structure of CYP106A2, UV–visible, CO-difference, CD and EPR spectra were recorded. The proteins were isolated in the oxidised, low spin state and showed peaks at 358, 417, 534 and 568 nm in the UV–visible spectra. These are similar values to the ones that were published by Berg et al., who characterised CYP106A2 for the first time.[5,43,44] For purified WT-CYP106A2, $\Delta\varepsilon_{417}$ of 120 $mM^{-1}cm^{-1}$ was determined and the haem content was 100%. The UV–visible spectra of all mutants were indistin-

```
α-L          β-3-3/β-4-1                β-4-2/β-3-2
CYP106A2 351 GPHFCLGAPLARLEAKIALTAFLKKFKHIEAVPSFQLEENLTDSATGQTLTSLPLKASRM 410
CYP11B1  446 GMRQCLGRRLAEVEMLLLLHHVLKHLQ-VETLTQEDIKMVYSFILRPSMFPLLTFRAIN  503
             * : ***  **.:*  : *  .**::: :*::.. :::   :     . :. *.::* .
```

Figure 5. Alignment between CYP106A2 and human CYP11B1 in the putative SRS6 region. The alignment was generated by using CLUSTAL W 1.8.[66] The absolutely conserved residues are highlighted in black boxes and marked by asterisks below the sequences. Conserved and highly conserved residues are marked by points or colons below the sequences, respectively. The secondary structure elements above the sequences are labelled according to Haseman et al.[22] The mutated residues are highlighted in grey. The numbering of CYP11B1 is shown for the unprocessed protein.

guishable from WT-CYP106A2, both in the oxidised and the reduced state (data not shown). The CO-difference spectra for all mutants exhibited absorption maxima at 450 nm; this attests to the correct incorporation of the haem (data not shown). The EPR spectra of WT-CYP106A2 and all mutants also showed characteristic signals for low-spin cytochrome P450s with signals at $g_1 = 2.426$, $g_2 = 2.248$ and $g_3 = 1.192$. The CD spectra for WT-CYP106A2 and all mutants in the far-UV region revealed no significant changes (Figure 6A). Because the CD spectra of proteins in this range reflect conformational changes of the backbone, the overall topology of the enzymes is apparently not affected by any of the mutations. CD spectra in the near-UV and visible region (300–450 nm) showed the typical W pattern, with minima at 350 and 409 nm representing the Delta and the Soret bands (Figure 6B). The Soret band splits up in the typical minimum at 409 nm and an extra band at 430 nm, which is not observed in other cytochrome P450s.[45–48] This region is slightly changed for the mutants in the putative SRS 6 region, which indicates changes in the haem environment in comparison to the wild type. The results from the UV–visible, difference, EPR and CD spectra in the UV region together provide evidence that all mutants were expressed as holoproteins with the haem situated similar to that of WT-CYP106A2, and with no structural disruption. In contrast, the CD spectra in the visible region indicate slight changes in the haem environment for the mutants in SRS 6.

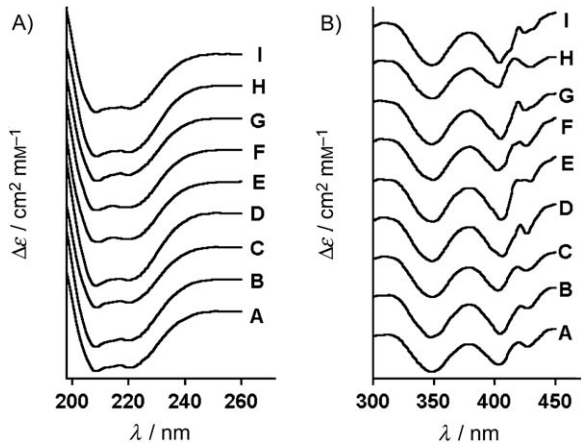

Figure 6. CD spectra of WT-CYP106A2 and the mutants. A) Far-UV region representing the backbone conformation of WT-CYP106A2 and the mutants. B) Near-UV and visible region representing the haem and its environment of WT-CYP106A2 and the mutants. All spectra were recorded at room temperature in 1-cm cuvettes. For the CD spectra in the far-UV region the enzyme concentrations were 0.5 μM in 2.5 mM phosphate buffer (pH 7.4). For the CD spectra in the near-UV and visible region the enzyme concentrations were 20 μM in 10 mM phosphate buffer (pH 7.4). The graphs are shifted along the x-axis for better comparison. a) WT-CYP106A2, b) E90V/D185G, c) K27R/I71T/I215T, d) I86T, e) S394I, f) A395L, g) T396R, h) G397P, i) Q398S.

Catalytic activity and regiospecificity of the mutants

By using DOC as a substrate, 15β-OH-DOC is the only product that is observed, both in the case of WT-CYP106A2 and all the mutants (except T396R). By using P as a substrate, 15β-OH-P is the main product of WT-CYP106A2 and all mutants (again except T396R); however, the 11α-, 9α- and 6β-hydroxylation varies substantially in the case of the central mutants in SRS 6. To compare the hydroxylation activities of WT-CYP106A2 and the mutants, K_M and V_{max} values for the 15β-hydroxylation of DOC and P have been determined by using various adrenodoxin concentrations (Table 3).

Table 3. Catalytic properties of WT-CYP106A2 and the mutants. For the 15β-hydroxylation activities, WT-CYP106A2 and the mutants were reconstituted by using a concentration of 300 μM P or 400 μM DOC, 0.25 μM cytochrome P450s, 0.50 μM adrenodoxin reductase and differing concentrations of adrenodoxin. The reactions were carried out at 30 °C for 3 min in a volume of 500 μL in 50 mM HEPES (pH 7.4) in presence of a NADPH-regenerating system. The products of the hydroxylation reaction were analysed by HPLC. The K_M and V_M values and their standard deviations were calculated from three independent experiments.

	15β-Hydroxylation activity			
	P		DOC	
	K_M [μM]	V_{max} [nmol min^{-1} per nmol CYP]	K_M [μM]	V_{max} [nmol min^{-1} per nmol CYP]
WT-CYP106A2	1.5 ± 0.5	233 ± 16	1.5 ± 0.2	246 ± 9
E90V/D185G	1.0 ± 0.4	205 ± 20	1.9 ± 0.6	208 ± 15
K27R/I71T/I215T	0.7 ± 0.3	276 ± 36	2.4 ± 0.8	265 ± 20
I86T	0.9 ± 0.3	280 ± 23	1.2 ± 0.4	254 ± 21
S394I	4.3 ± 0.7	89 ± 4	4.7 ± 1.4	46 ± 3
A395L	2.4 ± 0.4	186 ± 7	4.2 ± 1.2	104 ± 8
T396R	n.d.*	n.d.*	n.d.*	n.d.*
G397P	5.0 ± 0.9	15 ± 1	4.6 ± 0.8	5.3 ± 0.3
Q398S	4.9 ± 0.7	155 ± 5	5.6 ± 1.0	75 ± 3

n.d.*: not detectable.

In the case of DOC as a substrate, the V_{max} value of 15β-hydroxylation of WT-CYP106A2 was 246 nmol 15β-OH-DOC min^{-1} per nmol CYP106A2^{-1}. The V_{max} values of the mutants for which no participation in substrate binding was predicted varied only between 85% and approximately 110% of WT-CYP106A2. Also the K_M values were comparable to WT-CYP106A2. In the case of the mutants in SRS 6 region, the result was quite different. In this set, mutant A395L had the highest V_{max} value with only ~40% of the WT-CYP106A2 15β-hydroxylation activity, followed by Q398S with ~30% and S394I with ~20% of the wild-type activity. Mutant G397P exhibited only 2% of the wild-type activity, and T396R did not produce any hydroxylated product up to an adrenodoxin concentration of 100 μM. In the case of P, WT-CYP106A2 had a V_{max} value of 233 nmol 15β-OH-P min^{-1} per nmol CYP106A2^{-1}. The V_{max} values for the mutants showed a similar trend as for DOC, although the effect was less pronounced. For the mutants with no predicted effect (E90V/D185G, K27R/I71T/I215T and I86T) it

varied between 90% and 120% of the wild-type activity. For the mutants in SRS 6 the result was again remarkably different. As seen with the 15β-hydroxylation of DOC, mutant A395L was again the most active 15β-hydroxylase with 80% of the activity of WT-CYP106A2, followed by Q398S with 70% and S394I with 40% of the wild-type activity. Also very comparable to the DOC experiments, the 15β-hydroxylation activity of the G397P mutant was very low with only 6% of the WT-CYP106A2 activity, whereas again, mutant T396R did not produce any detectable products up to an adrenodoxin concentration of 100 μM.

In order to compare the regiospecificity of WT-CYP106A2 with the two sets of mutants, a representation of the product distribution of the 15β-, 11α-, 9α- and 6β-hydroxylation for P is shown on Figure 7. Figure 7A represents the absolute product formation of all monohydroxy-Ps produced, Figure 7B represents the relative product distribution when 15β-OH-P is set to 100%. At a concentration of 20 μM adrenodoxin, WT-CYP106A2 produces 160 nmol 15β-OH-P min^{-1} per nmol CYP. 11α-, 9α- and 6β-OH-P are produced at only 9, 4 and 9%, respectively. A comparable product distribution was observed for the three mutants E90V/D185G, K27R/I71T/I215T and I86T, for which no influence on substrate binding was predicted. Mutant E90V/D185G produced 150 nmol 15β-OH-P min^{-1} per nmol CYP and 11α-, 9α- and 6β-OH-P are produced at 15, 6.5 and 12.5% of the wild-type activity, respectively. The respective values for mutant K27R/I71T/I215T are 190 nmol 15β-OH-P min^{-1} per nmol CYP and 8, 4 and 8%, and for I86T 205 nmol 15β-OH-P min^{-1} per nmol CYP and 16, 6 and 13%. This means that only in the case of E90V/D185G and I86T was a small but perceivable increase in 11α- and 6β-hydroxylation observed. From the mutants in SRS 6 only the terminal mutants, S394I and Q398S exhibited a comparable hydroxylation profile to WT-CYP106A2. Mutant S394I produced 70 nmol 15β-OH-P min^{-1} per nmol CYP and 5, 4 and 5% of 11α-, 9α- and 6β-OH-P, respectively, and mutant Q398S produced 115 nmol 15β-OH-P min^{-1} per nmol CYP and 7, 3 and 7% of 11α-, 9α- and 6β-OH-P. The most dramatic changes in the hydroxylation profile were observed for the two central mutants in SRS 6, A395L and G397P. For mutant A395L, which produced 145 nmol 15β-OH-P min^{-1} per nmol CYP, the 11α-OH-P formation was increased to 39%, that of 9α-OH-P to 20%, whereas 6β-OH-P formation was relatively unchanged (7%). This is a more than fourfold increase in the relative 11α-hydroxylation activity and a fourfold increase in the relative 9α-hydroxylation. The absolute formation of 11α-OH-P increased therefore from 14 nmol 11α-OH-P min^{-1} per nmol CYP to 60 nmol 11α-OH-P min^{-1} per nmol CYP and that of 9α-OH-P from 6 nmol 9α-OH-P min^{-1} nmol CYP to 29 nmol 9α-OH-P min^{-1} per nmol CYP. This means that even the absolute formation of this mutant is increased more than four times in the case of 11α-OH-P and approximately five times in the case of 9α-OH-P. In the case of mutant G397P, the relative formation of 11α-OH-P is increased to 41%, followed by 6β-OH-P to 21% and 9α-OH-P to 9%. This also represents a more than fourfold increase in the relative 11α-hydroxylation activity, and a more than twofold increase in 6β-hydroxylation of P compared to WT-CYP106A2. However, the absolute product formation of mutant G397P is extremely low. Because only 11 nmol 15β-OH-P min^{-1} per nmol CYP 15β-OH-P are produced by this mutant, which is approximately 7% in comparison to WT-CYP106A2, the absolute formation of 11α-OH-P and 6β-OH-P is nevertheless lower than that of WT-CYP106A2. Taken together, it can be stated that, as predicted by the created computer model, the amino acid replacements in the variable regions on the surface of CYP106A2 had no significant effect on hydroxylation activity and selectivity, whereas in the case of replacements in SRS 6 the activity as well as the regiospecificity of the steroid hydroxylation were different.

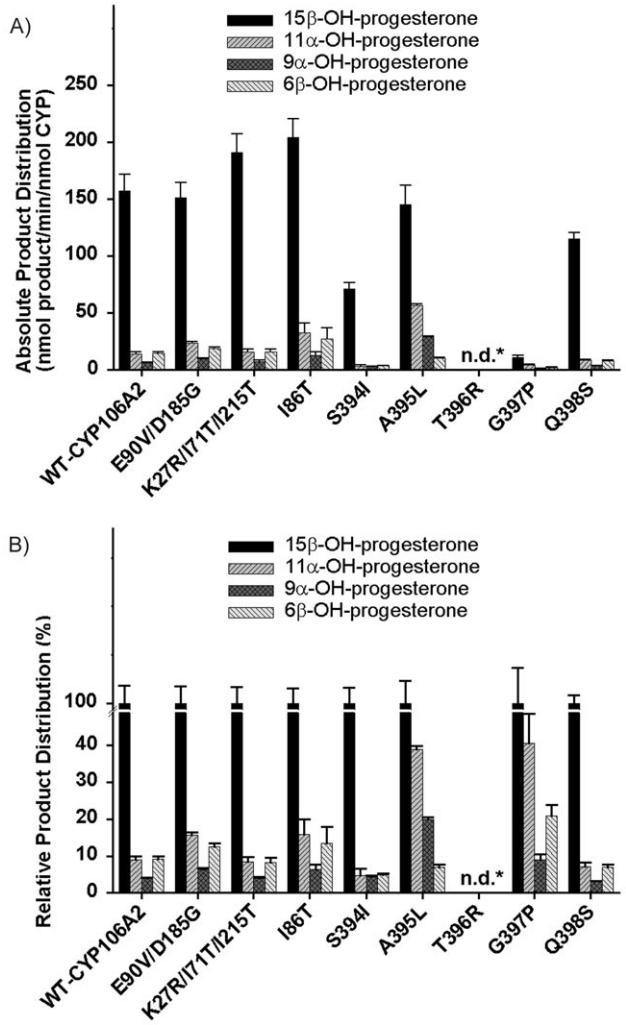

Figure 7. Representation of the A) absolute and B) relative product distribution of 15β-, 11α-, 9α- and 6β-OH-P produced by WT-CYP106A2 and the mutants (15β-OH-P is set to 100%). The reactions were carried out at 30 °C for 3 min in a volume of 500 μL in 50 mM HEPES (pH 7.4) in presence of a NADPH-regenerating system. The concentrations were 300 μM P, 0.25 μM cytochrome P450s, 0.50 μM adrenodoxin reductase and 20 μM adrenodoxin. The standard deviation corresponds to three independent experiments (n.d.*: not detectable).

Conclusions

By using the SYBYL 6.7 subroutine COMPOSER and five template cytochrome P450s a low homology model of CYP106A2 has been constructed. To assess the good quality and reliability of

the model, a thorough theoretical evaluation of the model was performed. Its stereochemical and energetic properties and the packing environment of its residues are comparable to those of the template proteins. The results showed that backbone and side-chain conformations, bond lengths and angles (PROCHECK), residue interaction (PROSA II) and residue contacts (WHATIF quality control) of the CYP106A2 model are well within the criteria that have been established for reliable structures, and are in part of almost as good quality as those of the reference proteins (Table 2, Figure 3). Predictions of the model about the haem charge neutralisation, catalysis and redox–partner interaction correlate well with features that are seen in other cytochrome P450 structures. For example the haem propionate charge neutralisation in the CYP106A2 model appears to be essentially homologous to the charge neutralisation that is found in CYP119 and many other structurally characterised cytochrome P450s. The finding that residues that are expected to be highly conserved in cytochrome P450 structures can be found at the corresponding positions in the CYP106A2 model proves that the alignment, the most crucial step in homology building, was reliable throughout the sequence. By using FLEXX, the substrate P could be docked into the active site with favourable energy scores. In the five favourable docking solutions with the lowest energy scores at least one hydrogen bond between the C3 keto group of P and the A395 to T396 loop could be observed; this indicates the importance of these residues for substrate orientation in the active site of CYP106A2 (Figure 4).

In order to evaluate the model experimentally, two sets of mutants have been created, expressed and analysed in detail. The first set comprises mutations for which no participation in substrate binding is predicted by the modelled enzyme–substrate complex. These six mutations are located in some of the most variable regions of cytochrome P450s and comprise the B′-helix and the F/G-loop. Both exhibit very different lengths and orientations as well as very low sequence identity among all structurally solved cytochrome P450s and are therefore the most tentative regions in cytochrome P450 homology modelling.[13,22,42] Mutations I71T, I86T, E90V align with the region around the B′-helix and D185G is situated in a putative substrate entrance channel region between helices F and G.[41] The second set contains mutations in SRS 6. The docked complex of CYP106A2 and the substrate P predicted an influence on substrate binding for the residues A395 and T396. Therefore, these residues and their nearer surrounding (S394, G397, Q398) were taken as candidates for the design of mutants to show their influence on the substrate binding experimentally. These residues were mutated to the corresponding ones that are found in the human 11β-hydroxylase CYP11B1.

The UV–visible, difference, EPR (data not shown) and CD spectra in the far-UV region (Figure 6A) of WT-CYP106A2 in comparison to all the mutants showed that the haem was inserted correctly, and that no major changes in the backbone conformation have occurred by the mutations. However, CD spectra in the near-UV and visible region (Figure 6B) of the mutants in SRS 6 gave rise to minor changes in the haem environment compared with WT-CYP106A2. This was already the first hint that active-site residues are involved in these mutants.

The K_M and V_{max} values for DOC and P hydroxylation as well as the product distribution of P hydroxylation have been determined for WT-CYP106A2 and were compared to both sets of mutants. In the case of the mutants E90V/D185G, K27R/I71T/I215T and I86T in which no effect on the activity was predicted by the model, the K_M and V_{max} values are in the same range as for WT-CYP106A2. In the case of the mutants S394I, A395L, T396, G397P, Q398S in SRS 6, where an influence on substrate binding was predicted, the V_{max} values were strongly reduced and the K_M values were partially dramatically increased, especially in the centre of this region (A395, T396, G397). In addition, the product distribution of P hydroxylation was dramatically changed for A395L and G397P (Figure 7). For mutant A395L, the amounts of 11α-hydroxylation and 9α-hydroxylation were increased fourfold and fivefold, respectively compared to WT-CYP106A2. The relative formation of 11α-OH-P by using mutant G397P was also more than four times higher, and the formation of 6α-OH-P was more than twofold increased in comparison to WT-CYP106A2. Mutant T396R did not show any catalytic activity in the enzyme-reconstituted assay up to an adrenodoxin concentration of 100 μM. This result was rather surprising because T396 is not a conserved residue at this position compared to other resolved cytochrome P450s.

The interesting point is that in the case of two mutants (A395L and G397P) mainly the 11-position of P hydroxylation was affected. Although the mutants have been derived by an alignment with the human 11β-hydroxylase CYP11B1, these two enzymes are only sparsely related (20% sequence identity). Although residue swapping experiments between cytochrome P450 families and subfamilies have been performed in the past, this has been mostly done for highly homologous cytochrome P450s. For example, by using the human CYP11B1 and CYP11B2 (93% sequence identity), the mutation of a single residue in the glucocorticoid-synthesising CYP11B1 conferred the mineralocorticoid-synthesising activity of CYP11B2 to CYP11B1,[49,50] and in reciprocal residue swapping experiments the mineralocorticoid-producing CYP11B2 could be converted to a glucocorticoid-producing enzyme with only two to three mutations.[51] In the case of slightly more distantly related cytochrome P450s, for example the progesterone 16α-hydroxylase CYP2B1 and the progesterone 21-hydroxylase CYP2C5 (~50% sequence identity), seven residue replacements were necessary to successfully confer CYP2B1 with 80% of the regiospecificity of progesterone 21-hydroxylation.[52]

A long-sought practical goal in cytochrome P450 research is to capitalise on the exquisite specificity of these enzymes in regio- and stereoselective hydroxylation reactions for the production of chemicals that are difficult to prepare by using traditional organic synthesis methods. This is especially true in the case of steroids, which are interesting pharmaceutical target substances for the production of anti-inflammatory, diuretic, anabolic, contraceptive, antiandrogenic, progestational and antitumour drugs. Therefore, the further development of CYP106A2 mutants that produce pharmaceutically interesting

steroids will be a challenging goal, and interesting for industries that are involved in their production. The tools that are described in this paper will certainly contribute to reach this goal.

Experimental Section

Reagents and chemicals: DOC and P were from Sigma Chemicals Co. (St. Louis, MO, USA). 11α-OH-P was from Steraloids Inc. (Newport, RI, USA). 6β-OH-P, 9α-OH-P 15β-OH-P and 15β-OH-DOC were a kind gift of the Schering AG (Berlin, Germany). All other chemicals were from standard sources and were of the highest purity available.

Modelling: The modelling has been performed on a Silicon Graphics O2 workstation by using the SYBYL 6.7 subroutine COMPOSER.[19] The amino acid sequence of CYP106A2 was taken from Rauschenbach et al.[53] The five template structures, namely CYP119 from *Sulfolobus solfataricus* (P450sulso, 1F4T),[42] CYP107A1 from *Saccharopolyspora erythrea* (P450eryF, 1OXA),[54] CYP108 from *Pseudomonas sp*. (P450terp, 1CPT),[55] CYP101 from *Pseudomonas putida* (P450cam, 1PHG)[56] and CYP55A1 from *Fusarium oxysporum* (P450nor, 1L6)[57] were obtained from the Protein Data Bank.[58] An alignment of all cytochrome P450s was produced by using the PMUTATION.HOMO similarity matrix.[19] Based on this alignment, the SCRs of the proteins were built; then, a protein loop search was done for the design of the SVRs. The SVRs were inspected visually and chosen according to minimal steric interactions with the surrounding parts of the protein, minimal root-mean-square distance for the fit and maximal sequence homology and similarity to the template cytochrome P450s. The F- and the G-helix were modelled by using WHATIF[59] as a modelling program and CYP107A1 (1OXA) as template, and then these fragments were fitted into the model of the whole protein. The structure was charged according to Gasteiger-Marsili,[60] and 100 steps of minimisation were performed by using the conjugate gradient algorithm and the TRIPOS force field.[61] The protein was then solvated with 5000 water molecules by using the algorithm XFIT,[19] and finally 300 minimisation steps in the presence of water were performed as described above. Further validation methods included PROCHECK,[62] PROSA II[20] and WHATIF.[21]

Docking and alignment with CYP11B1: Molecular docking calculations were performed for the substrate P. For the calculations, the FLEXX docking program was used.[63,64] The docked complexes were energy minimized for 5000 steps by using the steepest descent and conjugant gradient optimisation procedures within the GROMACS program and force field.[65] The alignment between CYP106A2 and human CYP11B1 in the SRS 6 region was created by using CLUSTAL W 1.8.[66]

Bacterial expression and purification of recombinant CYP106A2 and mutants: The CYP106A2 cDNA was a kind gift from Dr. Raimund Rauschenbach (Schering AG, Berlin, Germany). Expression of CYP106A2 was performed as described in Simgen et al.[67] Purification was performed according to Lisurek et al.[6]

Site directed mutagenesis: Mutagenesis of residues S394, A395, T396, G397 and Q398 was accomplished according to the protocol of the Quick Change Site-Directed Mutagenesis kit (Stratagene, La Jolla, CA, USA) by using oligonucleotide primers that were synthesised by MWG Biotech AG (Ebersberg, Germany) and the plasmid CYP106A2/pKKHC (NcoI/HindIII).[68] The three mutants I86T, E90V/D185G and K27R/I71T/I215T were obtained by using a modified plasmid CYP106A2/pKKHC (KpnI/SalIII). All mutations were confirmed by automatic sequencing by using a LiCor-4000 DNA sequencer (MWG Biotech AG).

Spectroscopic methods: Absorption spectra were recorded at room temperature on a Shimadzu double beam spectrophotometer UV2101PC (Kyoto, Japan). CO-difference spectra were recorded according to Omura and Sato.[69] The haem content was determined according to Schenkman and Jansson.[70] For the determination of the molar absorptivity, the absorption of CYP106A2 solutions with known protein concentrations (see below) were determined. Electron paramagnetic resonance (EPR) measurements were carried out on a Bruker ESP300E spectrometer (Billerica, MA, USA) at −196 °C in 50 mM K_3PO_4 (pH 7.4). Circular dichroism (CD) spectra were recorded on a Jasco J720 spectropolarimeter (Victoria, Canada). CD measurements at 195–260 nm were performed in 1 cm cuvettes that contained 0.5 μM cytochrome P450s in 2.5 mM K_3PO_4 (pH 7.4) and for measurements at 300–450 nm 20 μM cytochrome P450s in 10 mM K_3PO_4 (pH 7.4).

Catalytic activity and electron transfer: K_M and V_{max} values for increasing adrenodoxin concentrations were determined in a final volume of 0.5 mL at 30 °C for 3 min in 50 mM HEPES buffer, pH 7.4. The reconstituted system contained 0.5 μM adrenodoxin reductase, 0.25 μM cytochrome P450s, 400 μM DOC or 300 μM P as substrates, a NADPH-generating system as previously described,[6] and increasing adrenodoxin concentrations depending upon the mutant until the maximum substrate conversion was reached (in the case of DOC 10 μM WT-CYP106A2 and I86T, 20 μM E90V/D185G, K27R/I71T/I215T and A395L, 50 μM Q398S and 100 μM S394I, T396R and G397P were used, and in the case of P, 20 μM WT-CYP106A2, E90V/D185G, K27R/I71T/I215T and I86T, 50 μM A395L and 100 μM S394I, T396R, G397P and Q398S were used). Incubations were terminated and extracted with $CHCl_3$ (2×0.5 mL). The organic phases were collected and the solvent was evaporated. The steroid metabolites were redissolved in acetonitrile and applied to a reversed-phase Waters Nova Pak Nukleosil C_{18} (4 μm, 3.9×150 mm) column. HPLC experiments were carried out on a Jasco system that consisteed of a P4–980 HPLC pump, an AS-950 sampler, a UV-975 UV7 visible detector and a LG-980–02 gradient unit (Jasco, Groß-Umstadt, Germany) by using an isocratic solvent system that consisted of acetonitrile/H_2O (40:60). All mobile phases were degassed before use. The positions of the metabolites were identified by reference steroids; corticosterone was used as internal standard for the DOC experiments and 20β-OH-P was used as internal standard for the P experiments to exclude an uneven extraction of the steroids. To calculate the hydroxylation activity the relative amount of the products was determined by using the relative peak area of the internal standard. Data were fitted by hyperbolic regression by using Sigma Plot (Rockware, Golden, CO, USA).

To study the regiospecificity of P hydroxylation, the reactions and HPLC were conducted as described above by using the following mixture: 0.5 μM adrenodoxin reductase, 20 μM adrenodoxin, 0.25 μM CYP106A2 or the corresponding mutants, 300 μM P as substrate, and the NADPH-generating system described above. The HPLC patterns were compared to those with the corresponding standard compounds.

Other procedures: Protein concentrations were estimated by using the bicinchoninic acid method according to the method provided by the supplier (Uptima, Montluçon, France) and bovine serum albumin was used as a standard. Adrenodoxin reductase and adrenodoxin were heterologously expressed and purified according to Sagara et al. and Uhlmann et al., respectively.[71,72]

Abbreviations: CD, circular dichroism; CYP, Cytochrome P450, DOC, deoxycorticosterone; HEPES, [*N*-(2-hydroxyethyl)-piperazine]-*N*′-ethanesulfonic acid; P, progesterone; SCR, structurally conserved region; SRS, substrate recognition site; SVR, structurally variable region; WT: wild type.

Systematic nomenclature: progesterone, 4-pregnene-3,20-dione; corticosterone, 11β,21-dihydoxy-4-pregnene-3,20-dione; deoxycorticosterone, 21-hydroxy-4-pregnene-3,20-dione.

Acknowledgements

The authors thank Wolfgang Reinle for excellent purification of adrenodoxin reductase and adrenodoxin, Katharina Bompais and Natalie Lenz for DNA sequencing and Michael Ebelshäuser/Dr. Reinhard Kappl (Institute of Biophysics) for recording, processing and analysing the EPR spectra. R.B. is supported by the Fonds der Chemischen Industrie.

Keywords: cytochromes · hydroxylases · molecular modeling · mutagenesis · steroids

[1] D. R. Nelson, L. Koymans, T. Kamataki, J. J. Stegeman, R. Feyereisen, D. J. Waxman, M. R. Waterman, O. Gotoh, M. J. Coon, R. W. Estabrook, I. C. Gunsalus, D. W. Nebert, *Pharmacogenetics* **1996**, *6*, 1–42.
[2] P. R. Ortiz de Montellano in *Cytochrome P450: Structure, Mechanism and Biochemistry* (Ed.: P. R. Ortiz de Montellano), Plenum, New York, **1995**, pp. 245–303.
[3] R. Bernhardt, *Rev. Physiol. Biochem. Pharmacol.* **1996**, *127*, 137–221.
[4] A. Berg, J. Å. Gustafsson, M. Ingelman-Sundberg, K. Carlström, *J. Biol. Chem.* **1976**, *251*, 2831–2838.
[5] A. Berg, K. Carlström, M. Ingelmann-Sundberg, *Biochem. Biophys. Res. Commun.* **1975**, *66*, 1414–1423.
[6] M. Lisurek, M. J. Kang, R. W. Hartmann, R. Bernhardt, *Biochem. Biophys. Res. Commun.* **2004**, *319*, 677–682.
[7] G. W. Souness, D. J. Morris, *Hypertension* **1996**, *27*, 421–425.
[8] G. W. Souness, S. A. Latif, J. L. Laurenzo, D. J. Morris, *Endocrinology* **1995**, *136*, 1809–1812.
[9] J. Tamm, M. Seckelmann, U. Volkwein, E. Ludwig, *Br. J. Dermatol.* **1982**, *107*, 63–70.
[10] A. H. van der Willigen, J. D. Peereboom-Wynia, T. van Joost, E. Stolz, *Acta Derm.-Venereol.* **1987**, *67*, 82–85.
[11] C. Virus, M. Lisurek, B. Simgen, F. Hannemann, R. Bernhardt, *Biochem. Soc. Trans.* **2006**, *34*, 1215–1218.
[12] J. A. Braatz, M. B. Bass, R. L. Ornstein, *J. Comput.-Aided Mol. Des.* **1994**, *8*, 607–622.
[13] Y.-T. Chang, G. H. Loew, *Protein Eng.* **1996**, *9*, 755–766.
[14] Y. T. Chang, G. Loew, *Biochemistry* **2000**, *39*, 2484–2498.
[15] G. D. Szklarz, R. L. Ornstein, J. R. Halpert, *J. Biomol. Struct. Dyn.* **1994**, *12*, 61–78.
[16] G. D. Szklarz, J. R. Halpert, *Life Sci.* **1997**, *61*, 2507–2520.
[17] D. F. V. Lewis, *Xenobiotica* **1998**, *28*, 617–661.
[18] S. A. Usanov, S. E. Graham, G. I. Lepesheva, T. N. Azeva, N. V. Strushkevich, A. A. Gilep, R. W. Estabrook, J. A. Peterson, *Biochemistry* **2002**, *41*, 8310–8320.
[19] Sybyl 6.7, Tripos Inc., St. Louis, MO, 63144, USA.
[20] M. J. Sippl, *Proteins* **1993**, *17*, 355–362.
[21] G. Vriend, C. Sander, *J. Appl. Crystallogr.* **1993**, *26*, 47–60.
[22] C. A. Hasemann, R. G. Kurumbail, S. S. Boddupalli, J. A. Peterson, J. Deisenhofer, *Structure* **1995**, *3*, 41–62.
[23] R. Raag, S. A. Martinis, S. G. Sligar, T. L. Poulos, *Biochemistry* **1991**, *30*, 11420–11429.
[24] L. S. Koo, R. A. Tschirret-Guth, W. E. Straub, P. Moënne-Loccoz, T. M. Loehr, P. R. Ortiz de Montellano, *J. Biol. Chem.* **2000**, *275*, 14112–14123.
[25] L. S. Koo, C. E. Immoos, M. S. Cohen, P. J. Farmer, P. R. Ortiz de Montellano, *J. Am. Chem. Soc.* **2002**, *124*, 5684–5691.
[26] L. M. Geren, P. O'Brien, J. Stonehuerner, F. Millett, *J. Biol. Chem.* **1984**, *259*, 2155–2160.
[27] L. Geren, J. Tuls, P. O'Brien, F. Millett, J. A. Peterson, *J. Biol. Chem.* **1986**, *261*, 15491–15495.
[28] R. Bernhardt, A. Makower, G. R. Jänig, K. Ruckpaul, *Biochim. Biophys. Acta Protein Struct. Mol. Enzymol.* **1984**, *785*, 186–190.
[29] R. Bernhardt, K. Pommerening, K. Ruckpaul, *Biochem. Int.* **1987**, *14*, 823–832.
[30] V. M. Coghlan, L. E. Vickery, *J. Biol. Chem.* **1991**, *266*, 18606–18612.
[31] P. S. Stayton, S. G. Sligar, *Biochemistry* **1990**, *29*, 7381–7386.
[32] A. Wada, M. R. Waterman, *J. Biol. Chem.* **1992**, *267*, 22877–22882.
[33] T. C. Pochapsky, T. A. Lyons, S. Kazanis, T. Arakaki, G. Ratnaswamy, *Biochimie* **1996**, *78*, 723–733.
[34] H. Koga, Y. Sagara, T. Yaoi, M. Tsujimura, K. Nakamura, K. Sekimizu, R. Makino, H. Shimada, Y. Ishimura, K. Yura, M. Go, M. Ikeguchi, T. Horiuchi, *FEBS Lett.* **1993**, *331*, 109–113.
[35] K. Nakamura, T. Horiuchi, T. Yasukochi, K. Sekimizu, T. Hara, Y. Sagara, *Biochim. Biophys. Acta Protein Struct. Mol. Enzymol.* **1994**, *1207*, 40–48.
[36] M. Unno, H. Shimada, Y. Toba, R. Makino, Y. Ishimura, *J. Biol. Chem.* **1996**, *271*, 17869–17874.
[37] A. E. Roitberg, M. J. Holden, M. P. Mayhew, I. V. Kurnikov, D. N. Beratan, V. L. Vilker, *J. Am. Chem. Soc.* **1998**, *120*, 8927–8932.
[38] P. S. Stayton, T. L. Poulos, S. G. Sligar, *Biochemistry* **1989**, *28*, 8201–8205.
[39] D. F. V. Lewis, H. Moreels, *J. Comput.-Aided Mol. Des.* **1992**, *6*, 235–252.
[40] O. Gotoh, *J. Biol. Chem.* **1992**, *267*, 83–90.
[41] I. A. Pikuleva, A. Puchkaev, I. Björkhem, *Biochemistry* **2001**, *40*, 7621–7629.
[42] J. K. Yano, L. S. Koo, D. J. Schuller, H. Li, P. R. Ortiz de Montellano, T. L. Poulos, *J. Biol. Chem.* **2000**, *275*, 31086–31092.
[43] A. Berg, M. Ingelman-Sundberg, J. Å. Gustafsson, *J. Biol. Chem.* **1979**, *254*, 5264–5271.
[44] A. Berg, M. Ingelman-Sundberg, J. Å. Gustafsson, *Acta Biol. Med. Ger.* **1979**, *38*, 333–344.
[45] Y. L. Chiang, M. J. Coon, *Arch. Biochem. Biophys.* **1979**, *195*, 178–187.
[46] H. Hasumi, F. Yamakura, S. Nakamura, K. Suzuki, T. Kimura, *Biochim. Biophys. Acta Protein Struct. Mol. Enzymol.* **1984**, *787*, 152–157.
[47] L. A. Andersson, J. A. Peterson, *Biochem. Biophys. Res. Commun.* **1995**, *211*, 389–395.
[48] L. A. Andersson, A. K. Johnson, J. A. Peterson, *Arch. Biochem. Biophys.* **1997**, *345*, 79–87.
[49] B. Böttner, R. Bernhardt, *Endocr. Res.* **1996**, *22*, 455–561.
[50] B. Böttner, K. Denner, R. Bernhardt, *Eur. J. Biochem.* **1998**, *252*, 458–466.
[51] B. Böttner, H. Schrauber, R. Bernhardt, *J. Biol. Chem.* **1996**, *271*, 8028–8033.
[52] S. Kumar, E. E. Scott, H. Liu, J. R. Halpert, *J. Biol. Chem.* **2003**, *278*, 17178–17184.
[53] R. Rauschenbach, M. Isernhagen, C. Noeske-Jungblut, W. Boidol, G. Siewert, *Mol. Gen. Genet.* **1993**, *241*, 170–176.
[54] J. R. Cupp-Vickery, T. L. Poulos, *Nat. Struct. Biol.* **1995**, *2*, 144–153.
[55] C. A. Hasemann, K. G. Ravichandran, J. A. Peterson, J. Deisenhofer, *J. Mol. Biol.* **1994**, *236*, 1169–1185.
[56] T. L. Poulos, A. J. Howard, *Biochemistry* **1987**, *26*, 8165–8174.
[57] H. Shimizu, E. Obayashi, Y. Gomi, H. Arakawa, S. Y. Park, H. Nakamura, S. Adachi, H. Shoun, Y. Shiro, *J. Biol. Chem.* **2000**, *275*, 4816–4826.
[58] H. M. Berman, J. Westbrook, Z. Feng, G. Gilliland, T. N. Bhat, H. Weissig, I. N. Shindyalov, P. E. Bourne, *Nucleic Acids Res.* **2000**, *28*, 235–242.
[59] G. Vriend, *J. Mol. Graph.* **1990**, *8*, 52–56.
[60] J. Gasteiger, M. Marsili, *Org. Magn. Reson.* **1981**, *15*, 353–360.
[61] M. Clark, R. D. Cramer III, N. van Obdenbosch, *J. Comput. Chem.* **1989**, *10*, 982–1012.
[62] R. A. Laskowski, M. W. Arthur, D. S. Moss, J. M. Thornton, *J. Appl. Crystallogr.* **1993**, *26*, 283–291.
[63] M. Rarey, B. Kramer, T. Lengauer, *J. Comput.-Aided Mol. Des.* **1997**, *11*, 369–384.
[64] M. Rarey, B. Kramer, T. Lengauer, G. Klebe, *J. Mol. Biol.* **1996**, *261*, 470–489.
[65] E. Lindahl, B. Hess, D. van der Spoel, *J. Mol. Model.* **2001**, *7*, 306–317.
[66] J. D. Thompson, D. G. Higgins, T. J. Gibson, *Nucleic Acids Res.* **1994**, *22*, 4673–4680.
[67] B. Simgen, J. Contzen, R. Schwarzer, R. Bernhardt, C. Jung, *Biochem. Biophys. Res. Commun.* **2000**, *269*, 737–742.

[68] T. D. Porter, J. R. Larson, *Methods Enzymol.* **1991**, *206*, 108–116.
[69] T. Omura, R. Sato, *J. Biol. Chem.* **1964**, *239*, 2370–2378.
[70] J. B. Schenkman, I. Jansson in *Methods in Molecular Biology, Vol. 107, Cytochrome P450 Protocols* (Eds.: I. R. Phillips, E. A. Shephard), Humana, Totowa, NJ, USA, **1998**, pp. 25–33.
[71] Y. Sagara, A. Wada, Y. Takata, M. R. Waterman, K. Sekimizu, T. Horiuchi, *Biol. Pharm. Bull.* **1993**, *16*, 627–630.
[72] H. Uhlmann, V. Beckert, D. Schwarz, R. Bernhardt, *Biochem. Biophys. Res. Commun.* **1992**, *188*, 1131–1138.

Received: November 7, 2007
Published online on May 15, 2008

